Indian Journal of Pure & Applied Physics
Vol. 62, May 2024, pp. 363-371
DOI: 10.56042/ijpap.v62i5.6394

Diurnal Variation of Rain Drop Size Distribution over the Western Ghats of India

Amit Kumar[a,b], A K Srivastava[a]*, K Chakravarty[a] & Manoj K Srivastava[b]

[a]Indian Institute of Tropical Meteorology, Ministry of Earth Sciences, New Delhi 110 060, India
[b]Department of Geophysics, Banaras Hindu University, Varanasi 221 005, India

Received 25 October 2023; accepted 12 February 2024

Joss-Waldvogel Disdrometer (JWD) measurements at the High-Altitude Cloud Physics Laboratory (HACPL: 17.56°N, 73.4°E, above 1373 m MSL), Mahabaleshwar were investigated for determining the diurnality of the drop size distribution (DSD) associated with the precipitation characteristics over the Western Ghats of India. The JWD data for the period from 2015 to 2019 were collected and examined during the Indian Summer Monsoon (ISM) season. The number concentration of rain droplets of various diameters is considerably varying with the rain rate (R) and type of precipitating cloud. With increasing the value of R, rain droplets having larger diameter concentration significantly increases, and the distribution tail moves towards the biggest droplets. The average value of reflectivity (Z), R, liquid water content (LWC), mass-weighted mean diameter (D_m), and normalized intercept parameter ($\log_{10}N_w$) was found to be higher for the heavy rainfall ($R_{high} \geq 10$ mm h^{-1}) as compared to the low rainfall ($R_{low} < 10$ mm h^{-1}) during the entire study period. The gamma distribution of DSD shows significant differences during the low and heavy precipitation on different time periods (*e.g.*, 00-06, 06-12, 12-18, 18-23 LST). The number of rain events contributing to the total accumulated rain varies with time. The maximum number of rain events occurred during 12-18 LST, with 23.6 % rain events of low rainfall and 4.9% of heavy rainfall. The bimodality is observed in the diurnal variation of D_m, R, and Z, with the largest peak recorded in the late afternoon hour (13-16 LST) and the second crest in the early morning hour (05 LST). At the same time, the $\log_{10}N_w$ value drops down, indicating the lowest concentration of rain droplets.

Keywords: Disdrometer; Diurnal; Rainfall; DSD; Western ghats

1 Introduction

Rain droplet dimension and falling velocity is used to investigate the microphysical characteristics of different categories of the precipitating clouds[1]. The primary purpose of a disdrometer[2] is to provide the number of raindrops according to their diameter, from which the drop size distribution (DSD) is determined. Microphysical processes such as melting, condensation, break-up, collision-coalescence, riming, and ice formation greatly influence the DSD characteristics by amending cloud drops into rain droplets conversion process[3]. Knowledge about the DSD is necessary for microphysical parameterization in numerical cloud models and for determining the rain-integral parameters, like rain rate (R) and reflectivity (Z). The value of R with high accuracy can be determined by land-based instruments like rain gauges and disdrometer, which are used to calibrate and validate weather radars. Besides the rain rate, the disdrometer-derived DSD parameters have applications in improving the accuracy of a weather radar's quantitative precipitation estimation (QPE) algorithm[4], microphysical properties of rain, and erosion of regional soils[5].

Significant variations in the observed DSD characteristics have occurred with the latitude, season, cloud type, and rain rate[6]. Based on the disdrometer observation, we can classify cloud types into stratiform and convective clouds using the Z and R relationship[6], droplets concentration, and their sizes[7]. In both types of precipitating clouds, considerable spatial and temporal variations in the associated rain-integral parameters has been reported[8,9]. Sometimes stratiform and convective precipitation can be produced at different times and locations by a single cloud system[10]. It happens when the contribution of various microphysical processes has temporal and spatial variation in any precipitating cloud. The splitting of rain droplets acts as the primary microphysical process, and its enlargement through weak coalescence as a secondary process in stratiform precipitation. The slower rate of vertical circulation coupled with weak and extended large-scale vertical movement favours the development of stratiform precipitation. However, in convective precipitation, the periodic motion of convective clouds in the

*Corresponding author: (E-mail: atul@tropmet.res.in)

upward and downward direction and vertical circulation instantly enhance collision-coalescence and condensation processes, causing an increment in the concentration of bigger rain droplets and moisture content[10]. On the windward side of the Western Ghats, the complex mountainous structure imposes additional forcing on the clouds, resulting in deeper and more active clouds compared to surrounding areas[11]. Different classes of precipitating clouds (stratiform, convective, shallow-convective, and mixed-phase) were examined using the disdrometer and radar observations along the windward side of the Western Ghats[12]. They find that about 89% of rainfall originates from shallow convective precipitation, while the stratiform precipitation contribution is about 9%.

The rain droplets are the results of complex microphysical processes, and their spatial and temporal variation related to the precipitating cloud in terms of DSD has already been investigated worldwide and reported in various studies[6–8]. Several studies in the past based on the disdrometer and radar observations have been performed over the Indian region to understand the microphysical structure of the precipitating clouds[11,12,21,22]. Due to the complex mountainous structure of the Western Ghats along the west coast of India, the characteristics of rainfall are different and vary with the site[22]. An investigation of seasonal rain at Mahabaleshwar in the northern region of the Western Ghats, shows distinct DSD characteristics in the pre-monsoon, monsoon, and post-monsoon seasons[21]. A significantly high concentration of smaller rain droplets was observed in the monsoon and dominance of bigger rain droplet in the pre-monsoon season. The fluctuation of DSD with rain rate and season is occurred due to the difference in the microphysical processes and the influence of complex orography of the region. To understand the temporal variability of rainfall over the mountainous area, however, it is vital to understand the diurnal fluctuation of DSD. An investigation is required to understand the connections between the diurnal variation of DSD and atmospheric processes governing the regional weather and climate of the Western Ghats. The diurnal variation of DSD will aid in explaining the microphysical processes occurring within the precipitating cloud. It is helpful in parameterizing the microphysical aspects of the cloud in different numerical models. In the present study, the diurnal variation of DSD is determined at Mahabaleshwar over the Western Ghats of India, and investigated the potential factors responsible for it.

2 Data and Methodology

2.1 Study Location

In the Western Ghats region, the average altitude is around 800m above the mean sea level (MSL), and the slope varies between 5^0 and 20^0. The Arabian Sea, a significant source of moisture, is located on the west side of the Western Ghats; and a vast plain landmass is present on the east side. A permanent observation site was established at Mahabaleshwar for investigating the precipitating cloud structure and aerosol-cloud interaction. The site is known as High Altitude Cloud Physics Laboratory (HACPL: 17.56°N, 73.4°E, above 1373 m MSL) under the preview of the Indian Institute of Tropical Meteorology, Pune and located at an aerial distance of about 65 km.

2.2 Joss-Waldvogel Disdrometer

To study the diurnal variation of DSD, an impact-based disdrometer, *i.e.*, Joss-Waldvogel Disdrometer[2] (JWD) measurements were used during the Indian Summer Monsoon (ISM: June, July, August, and September month) period between 2015 and 2019 collected at the HACPL, Mahabaleshwar, which is situated in the windward side of the Western Ghats in India. The instrument is built by a Swiss company, Distromet Ltd, Switzerland. It works on the principle of electrical impulse and measures the number of rain droplets in 20 different-size bins ranging between 0.359 and 5.50 mm. It is to be noted here that the rain droplets less than 0.359 mm diameter is recorded as noise and a droplet diameter greater than 5.5 mm is registered in the bin where the biggest possible rain droplets are recorded. During the rain event, raindrop of various sizes collides with the sampling surface, styrofoam placed in an open area with dimension A, 50 cm^2, produces an electrical impulse depending upon the diameter and terminal velocity. JWD counts the number concentration of rain droplets in different size bins at an interval of 1 minute with an error[23] of ±5%, corrected by the dead time correction. However, no dead time correction[9] was applied to the JWD measurement, as correction is about 3% only.

If n_i is a number of raindrops of diameter D_i in the size bin, i recording it at time t. Then, the total number concentration $N(D_i)$ ($m^{-3}mm^{-1}$) of raindrop at any instant is given as:

$$N(D_i) = \sum_{i=1}^{20} {}^{n_i}/_{A * t * \Delta D_i * V(D_i)} \cdot \quad \ldots (1)$$

The velocity by which raindrops fall downward toward the earth's surface is known as the terminal velocity, represented by the symbol $V(D_i)$ (m sec^{-1}). The values of Z ($mm^6\ m^{-3}$) and R (mm h^{-1}) are directly proportional to the sixth and third power of the droplet's diameter, respectively. Using the $N(D_i)$, we can determine the total number concentration (N_t: m^{-3}), Z, R, and liquid water content (LWC: g m^{-3}) using the mathematical formula:

$$N_t = \sum_{i=1}^{20} N(D_i) * \Delta D_i \quad \text{... (2)}$$

$$Z = \sum_{i=1}^{20} N(D_i) * {D_i}^6 * \Delta D_i \quad \text{... (3)}$$

$$R = 6\pi * 10^{-4} \sum_{i=1}^{20} N(D_i) * V(D_i) * {D_i}^3 * \Delta D_i \quad \text{... (4)}$$

$$\text{and } LWC = \frac{\pi * \rho_\omega}{6000} \sum_{i=1}^{20} N(D_i) * {D_i}^3 * \Delta D_i \quad \text{... (5)}$$

ρ_ω (kg m^{-3}) is denoting the density of water.

The mass-weighted mean diameter (D_m: mm) is derived using the fourth and third order of moment:

$$D_m = \frac{\int_{min}^{max} D^4 N(D) dD}{\int_{min}^{max} D^3 N(D) dD} \quad \text{... (6)}$$

Using the parameters LWC and D_m, the mathematical formula of the normalized intercept parameter, N_w ($m^3\ mm^{-1}$), is

$$N_w = \frac{4^4}{\pi * \rho_\omega} \left(\frac{LWC}{D_m}\right) \quad \text{... (7)}$$

2.3 European Re-analysis-5 (ERA-5)

The ERA-5 is the latest (5th generation) reanalysis data[24] product of the European Centre for Medium-Range Weather Forecasts (ECMWF), archived at the data server under environmental services by the Copernicus Climate Change Service (C3S). This global data is critical for comprehending the microphysical and dynamical aspects of past events. In the current study, we utilized reanalysis data of the convective available potential energy (CAPE: J/kg), relative humidity (RH: %), u-component wind, and v-component wind at the spatial resolution of $0.25^0 \times 0.25^0$ in the surrounding region of HACPL. The data can be downloaded for the study region (Mahabaleshwar in the Western Ghats) from the C3S data server (https://cds.climate.copernicus.eu/cdsapp#!/home).

3 Results and Discussion

The average of RH and wind based on the ERA5 data during the ISM period over the Western Ghats, Arabian Sea, and their surrounding for the year 2015-2019 is shown in Fig. 1. The wind is blowing from the Arabian Sea toward the Western Ghats, paralleling the south-west monsoon movement. Warm and moist clouds from the Arabian Sea are mainly responsible for the rainfall over the Western Ghats. The value of RH is about 90 % in the monsoon season. The process of convection into precipitating clouds travelling from the Arabian Sea to the Western Ghats gradually increases with the mountain's altitude and slope[11].

3.1. Characteristics of Rain-Integral Parameters

Over the Indian region, the Indian Summer Monsoon (ISM) produced 70% of the total accumulated rain (https://imdpune.gov.in). The Western Ghats receive about 5,000 mm yearly accumulation of rain. JWD is an appropriate surface-based instrument for understanding DSD characteristics at the instrument site.

Figure 2 represents the histogram and cumulative frequency of Z, $\log_{10}R$, D_m, and $\log_{10}N_w$, based on the observed DSD from the JWD. Around 80 % of rain events occurred at the Mahabaleshwar during the ISM period, with the rain rate lying between 0.1-10 mm h^{-1}, as seen in Fig. 2(a). Less than 20% of rain events are the source of heavy precipitation (R ≥10 mm h^{-1}), following low and heavy orographic precipitation criteria[11]. Out of all rain events, two-thirds of rainfall produced reflectivity less than or equal to the 35 dBZ (Fig. 2(b)). The reflectivity produced by any precipitating cloud depends on the number concentration and size of rain droplets. Most of the

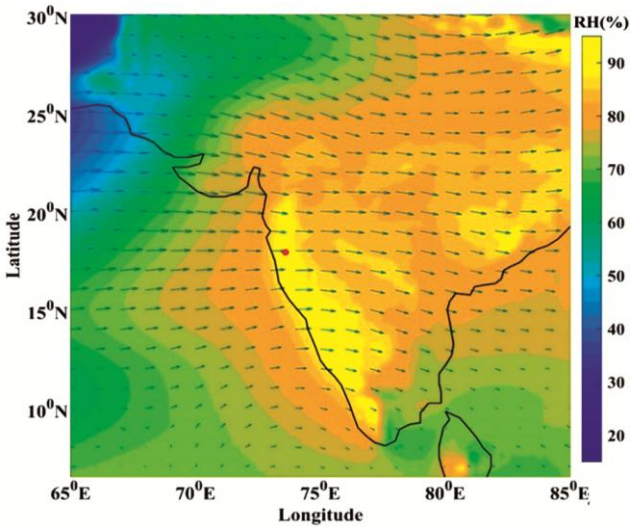

Fig. 1 — Mean of the relative humidity (RH: %) and wind direction in the surrounding region of HAPCL, Mahabaleshwar (shown by red dot), based on the ERA5 monthly data from 2015 to 2019.

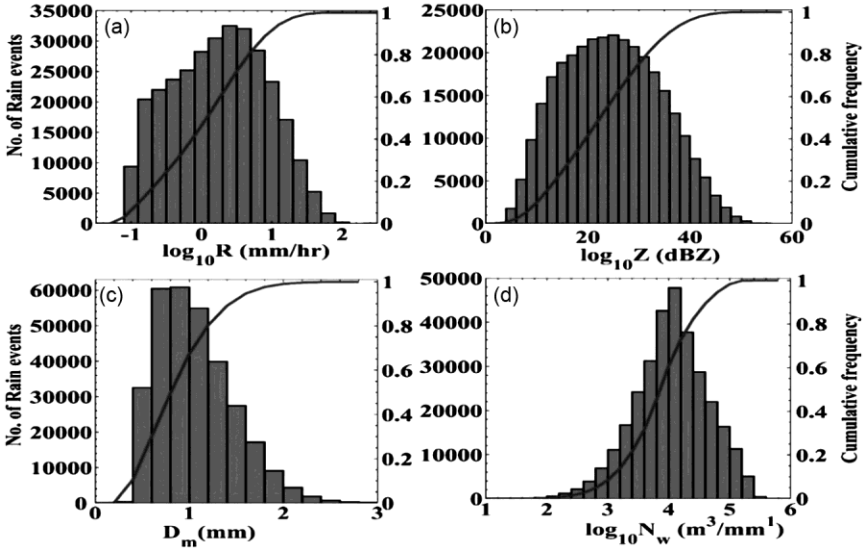

Fig. 2 — Histogram and cumulative distribution (red colour line) of (a) rain rate, (R: mm h^{-1}), (b) Reflectivity, (Z: dBZ), (c) mass-weighted mean diameter, (D_m: mm), and normalized intercept parameter, ($\log_{10}N_w$: (m^3 mm^{-1})) for the total 310263 rain events observed in the monsoon season from 2015 to 2019.

Table 1 — The mean value of rain-integral parameters for the seven different rain rate groups.

Category	No. of Samples	R (mm h^{-1})	LWC (g m^{-3})	Z (dBZ)	D_m (mm)	$\log_{10}N_w$ (m^3 mm^{-3})	N_t (m^{-3})
R1	75385	0.26	0.02	4.87	0.79	3.75	266
R2	39190	0.73	0.06	11.13	0.87	4.03	587
R3	44973	1.46	0.12	15.23	0.94	4.15	887
R4	64148	3.27	0.23	20.43	1.06	4.22	1208
R5	40985	7.11	0.43	26.24	1.26	4.18	1413
R6	41680	18.36	0.91	33.25	1.6	4.06	1530
R7	3902	53.85	2.22	42.27	2.2	3.89	1702

DSD measuring instruments sample the smaller rain droplets with less accuracy as compared to the bigger rain droplets. To overcome this shortcoming of the DSD measuring instrument, the size of the droplets is derived by dividing the M_4 (fourth moment) with the M_3 (third moment) of the DSD, which is commonly known as the mass-weighted mean diameter (D_m). According to Fig. 2(c), the peak of the D_m is around 1 mm, and the cumulative frequency indicates that most of the rain droplets are less than 2 mm in diameter. The number concentration of rain droplets gradually increases with the $\log_{10}N_w$ values, and the pinnacle point is around 4.2 mm, as shown in Fig. 2(d).

3.2. Characteristics of DSD under different rain rates

All the observed rain events are sorted according to the rain rate, which has been divided into seven different groups (R1, R2, R3, R4, R5, R6, and R7) as per the classification conditions[21]. The rain-integral parameters related to each group are given in Table 1. The number of rain events is maximum in group R1 with a rain rate between 0.1- 0.5 mm h^{-1} and the least in R7 group, containing rain events having R> 40 mm h^{-1}. The mean values of N_t, D_m, R, and LWC gradually increase and reach the highest value from R1 to R7 group. Light rainfall occurs for a longer duration with lower accumulated rainfall, while intense rainfall for a shorter duration produces the highest accumulated rainfall.

The gamma distribution associated with each group of rain events is plotted in Fig. 3, representing the average concentration of rain droplets of various diameters. The spectrum varies depending on the group of rain rate. For group R1, the average spectrum is narrower as compared to the others. With the increasing order of the group, the distribution is becoming broader. The gamma distribution's tail is shifting toward the rain droplets of large diameter up to R3. Furthermore, the average concentration of rain droplets with a fixed diameter is considerably increasing with the rain rate. The R7 group has maximum broadness and is highly distinct compared

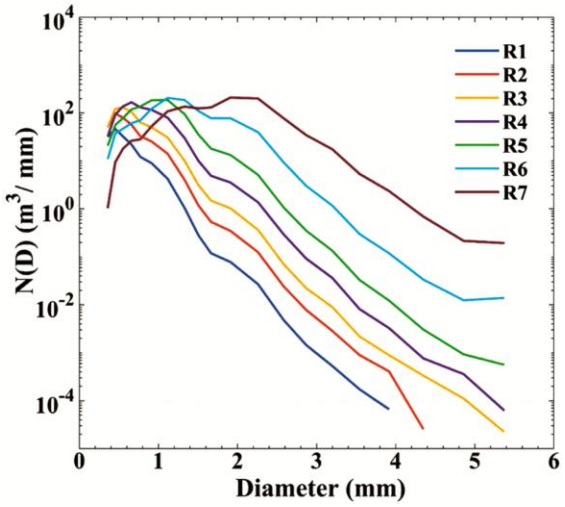

Fig. 3 — Relationship between number concentration (N(D)) and diameter for the different rain rate groups during the Indian Summer Monsoon season at the Mahabaleshwar.

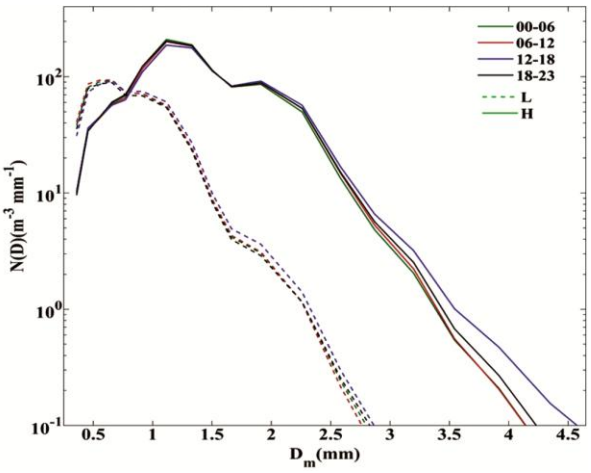

Fig. 4 — Gamma distribution for the low (R < 10 mm h^{-1}) and heavy (R ≥ 10 mm h^{-1}) rainfall during the Indian Summer Monsoon for the different time intervals as 00-06, 06-12, 12-18, and 18-23 LST (shown in different colors). Low (L) and Heavy (H) rainfall is denoted by dotted and solid lines, respectively.

to the gamma distribution of other groups. The microphysical properties of the orographic precipitation over the Western Ghats during the low (L: R_{low} < 10 mm h^{-1}) and heavy (H: R_{high} ≥10 mm h^{-1}) precipitation are found to be different[11]. The Arabian Sea is along the west side of the Western Ghats, which provides an enormous amount of moisture to the clouds passing over it. When these precipitating clouds, with vast moisture content, travel to the Western Ghats, they provide high accumulated rainfall over the region. The rate of microphysical process occurring in these precipitating clouds significantly increases due to the Western Ghats' complex topography. The process of collision-coalescence is enhanced, and the breaking-up process diminishes during heavy precipitation.

For understanding the diurnal variation of DSD in the monsoon season, the relation between the number concentration of rain droplets and their diameter during the low (L) and heavy (H) precipitation are estimated for the different local standard time (LST) intervals (00-06, 06-12, 12-18, and 18-23). Fig. 4 shows significant variations in DSD parameters depending on the rain rate and different time intervals. The average spectrum for the two different groups of rain rate considerably varies irrespective of an interval of time. However, during the 12-18 LST, the distribution tail extends to giant rain droplets in diameter, aligning with the formation of a convective cloud in the areas. The concentration of bigger rain droplets increases with the convective clouds present in the morning and afternoon time. On the other hand,

Table 2 — Percentage of low and heavy precipitation occurred in different time intervals.

Time (LST)	Low (R< 10 mm h^{-1}) (in %)	Heavy (R ≥ 10 mm h^{-1}) (in %)
00-06	20.2	3.1
06-12	19.7	3.3
12-18	23.6	4.9
18-23	21.8	3.4

the spectra show a small deviation at night-time (18-23 LST) compared to the morning and afternoon spectra, with relatively more rain droplets (diameter > 4 mm). It may possibly be due to the presence of a convective cloud in the evening, which is later dissipated. Rain droplets of diameter less than 3 mm during the light rainfall are observed for all the time intervals, signalling poor linkage between the rain rate group and the size of droplets. Table 2 provides the contribution of low and heavy precipitation for the different time intervals. Around 28.5% of the total rain events occurred between 12-18 LST, containing the biggest droplets and high concentrations of different diameters of rain droplets. The rainfall over the Western Ghats in the monsoon season mainly happens due to the large-scale circulation and orography effect. It may be one of the possible reasons for the small variation in the number of rain events and total accumulated rainfall observed in the 6-hourly diurnal distribution. For example, the lowest number of rain events (22.6%) happened in the 06-12 LST, while in the 00-06 LST, only 0.4% more rain events occurred compared to the 06-12 LST.

3.3 Characteristics of DSD in different cloud types

Stratiform clouds are mainly responsible for the Western Ghats' rainfall during the ISM season, but some convective precipitation also occurs, which causes an intense category of rainfall over the region[21]. JWD measurement classified the precipitating cloud into convective and stratiform[7], using R as a classification parameter. In the 10 min continuous rainfall, if the mean and standard deviation of R is more than 5 and 1.5 mm h^{-1}, respectively, the rain is assumed to be caused by the convective cloud, otherwise stratiform origin. The spectrum for both types of precipitating clouds during the ISM is shown in Fig. 5. On the left side of the 1 mm diameter, the mean concentration of rain droplets is high for the stratiform cloud as compared to the convective cloud; however, vice-versa was observed for drop diameter > 1 mm. The difference in concentration between the two types of precipitating clouds grows as droplet diameter increases. The number of bigger rain droplets gradually decreases (increases) during the stratiform (convective) precipitation. It may occur due to the dominance of different microphysical processes in the stratiform and convective clouds[21]. The number of rain events related to the convective cloud is around 27%, which is much less than the stratiform cloud (~68%), but it is pivotal for determining the governing microphysical process. The derived mean of R, Z, and D_m is larger for the convective precipitation than the corresponding value related to the stratiform precipitation.

The slope of gamma distribution is maximum for stratiform precipitation compared to the convective precipitation, with a considerable concentration of bigger rain droplets. It is happening due to the process of collision-coalescence, which is responsible for the formation of bigger rain droplets. While the disintegration of bigger rain droplets due to the break-up process in the stratiform precipitation increases the concentration of smaller rain droplets. As a result no rain droplets were observed for a diameter greater than 4 mm.

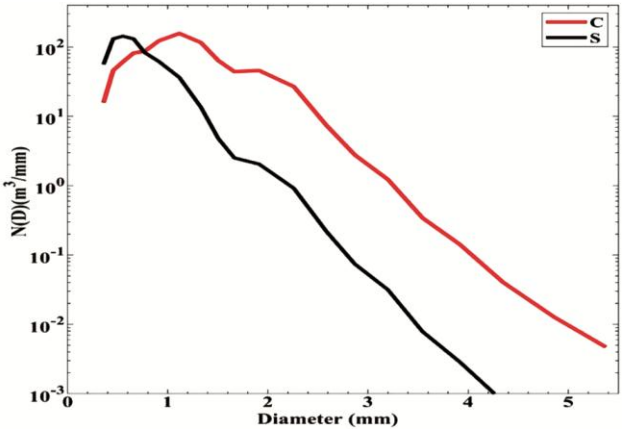

Fig. 5 — N(D) vs. rain droplet's diameter (mm) for the convective (C, represented with a red line) and stratiform (S, represented with a black line) precipitation.

Figure 6 represents the probability density function (PDF) of D_m and $\log_{10}N_w$ related to the convective (C) and stratiform (S) precipitation. The D_m shows a unimodal distribution for both convective and stratiform precipitation (Fig. 6(a)). However, relatively broader distribution is found to be associated with the convective precipitation as compared to the stratiform precipitation. From the PDF of $\log_{10}N_w$ (Fig. 6(b)), the bimodal distribution is observed for the stratiform; however, the convective precipitation has only a single peak at about 2 m^3 mm^{-1}. It may be inferred that the robust microphysical processes are occurring in the convective cloud, increasing the concentration of rain droplets having larger diameters and simultaneously decreasing the concentration of smaller rain droplets. The rate of splitting of rain droplets is high compared to the lower rate of coalescence, possibly occurring in stratiform precipitation. The considerably high concentration of small rain droplets for the stratiform rain is positively confirming from Fig. 6(a).

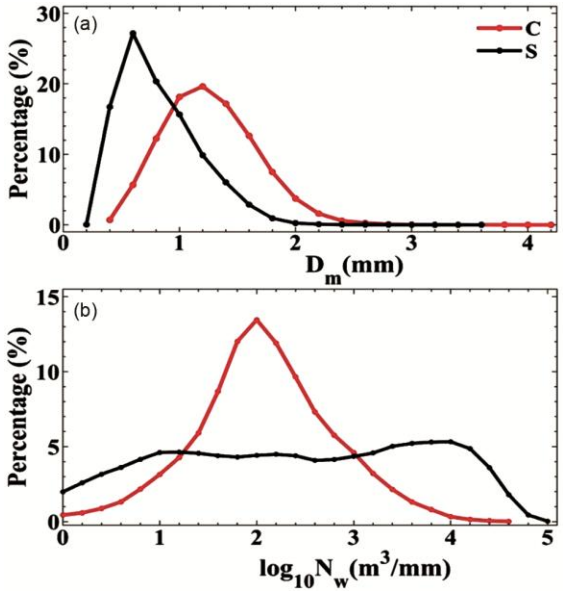

Fig. 6 — Probability Density Functions (PDF) of the (a) mass-weighted mean diameter, D_m (mm), and (b) normalized intercept parameter, $\log_{10}N_w$ (m^3 mm^{-1}) for the convective and stratiform precipitation.

3.4 Diurnal variability in DSD

Figure 7 represents the diurnal variation of the rain-integral parameters, e.g., R, Z, $D_{m,}$ and $\log_{10}N_{w,}$ using all the DSD observations. All the rain-integral parameters, except $\log_{10}N_{w,}$ demonstrate bimodal distribution, with one small peak in the morning time around 5 LST and the highest peak observed between 13-16 LST. It is also observed that the $\log_{10}N_w$ reaches its lowest values simultaneously (Fig. 7(d)), which is likely to be caused by a developed convective cloud with significant concentrations of rain droplets of larger diameter. The microphysical process like collision-coalescence, riming, and melting happening inside the convective clouds may decrease the value of $\log_{10}N_w$ and form rain droplets of larger diameter, supported by the diurnal variation of D_m, as given in Fig. 7(c). In a recent study, Sumesh et al. (2021)[13] also investigated the variations in cloud properties over the Western Ghats and coastal areas using the ceilometer, disdrometer, and satellite observations. They find that mid-level clouds are primarily causing the diurnal variation of rainfall. Strong CAPE and high liquid water content in the monsoon season are responsible for the widespread formation of stratiform clouds in the mountainous region. Several other researchers have also investigated the precipitation microphysics of the Western Ghats using in-situ[14–19] and satellite[20] measurements. Convective storms forming over the Western Ghats are examined using the surface-based X-band radar measurement coupled with TRMM (Tropical Rainfall Measurement Mission) satellite observation during the ISM[25]. According to their study, compared to other times of day, the likelihood of a convective storm forming is relatively high during the early morning and late afternoon time. It is consistent with the reported bimodal distribution of Z, R, D_m, and $\log_{10}N_w$ in the present study. The value of rain-integral parameters is maximum at the time of 5 LST and between 13-16 LST periods of an occurrence of convection. Surface wind convergence, radiative heating and cooling fluctuation, and the surrounding topography effects are likely responsible for the diurnal cycle.

When a cloud system moves from the Arabian Sea and reaches the top of the mountainous region, it simultaneously gets uplifted in the upward direction due to the orography, and alteration in the rain droplets formation occurs[11]. The Arabian Sea is a large water body with considerable heat storage capacity compared to the surrounding land mass, such as the Western Ghats. Due to the uneven heat storage capability between two-surrounding regions, the direction of wind movement is opposite during the day and night times[26]. In the daytime, the availability of high solar radiation causes heating of both regions, but the Western Ghats get heat in the least time due to the low heat capacities as compared to the Arabian Sea. The air nearer to the top layer of the mountainous region becomes warm, creating a low-pressure area

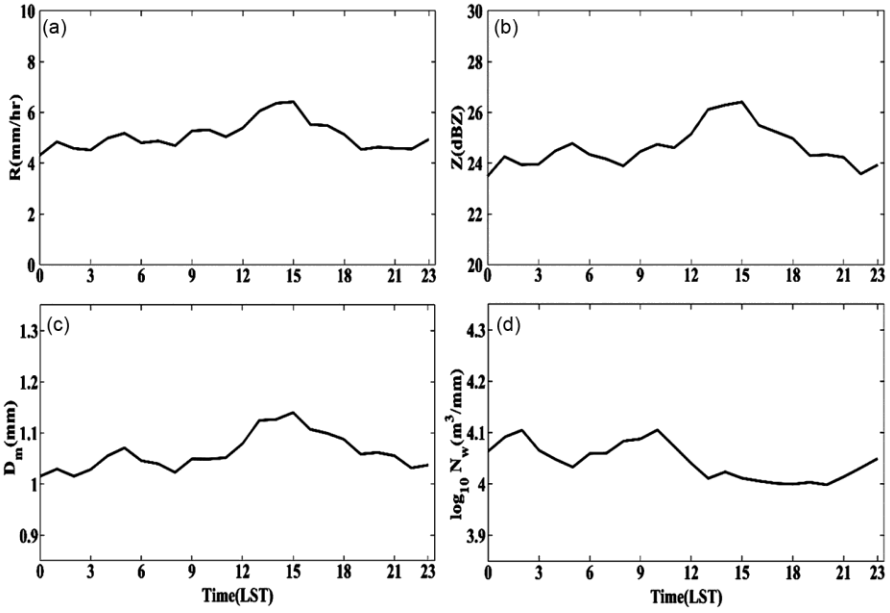

Fig. 7 — Diurnal Variation of the (a) rain rate (R: mm h^{-1}), (b) reflectivity (Z: dBZ), (c) mass-weighted mean diameter (D_m: mm), and (d) normalized intercept parameter ($\log_{10}N_w$: m^3 mm^{-1}).

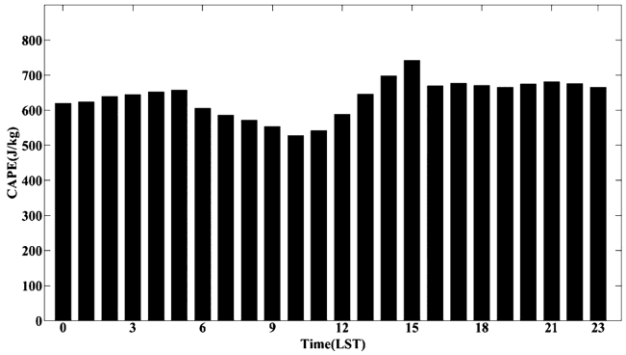

Fig. 8 — Hourly distribution of the convective available potential energy (CAPE: J kg^{-1}).

and moving upward. The dense cold air from the high-pressure region above the Arabian Sea started moving toward the Western Ghats, forming a complete cycle of circulation of air known as land breeze. While at night, the direction of the wind gets reversed, and it starts flowing from the Western Ghats toward the Arabian Sea. Other than the land-sea breeze, the diurnal variation of surface reaching solar radiation and topography of the Western Ghats are also responsible for rainfall variation at time of the day. Due to the complex terrain of the Western Ghats, having unevenly heated surface amend the various microphysical processes of the precipitating cloud. The combined effects of land-sea breeze, available solar radiation at any time of day, and complex topography of the Western Ghats are responsible for the diurnal variation of DSD.

To further support this, the hourly distribution of the average CAPE (Convective Available Potential Energy) over the region has been studied and shown in Fig. 8. The average CAPE distribution follows the diurnality of rain-integral parameters. The occurrence of one small peak in the morning time around 5 LST is different from late afternoon time peak at 15 LST. The slight fluctuation in the spectra of the rain-integral parameter in the morning is a possible reason for it, when the stratiform cloud is present above the Western Ghats. The observed R value is lower as compared to the afternoon rainfall, containing significant rain droplets with diameter less than 1 mm. The presence of the stratiform is responsible for the light rainfall and vigorous occurrence of the breaking-up process, increasing the concentration of smaller droplets. Due to the sunrise, the amount of solar radiation starts increasing with time. The initiation process occurring in the stratiform and convective cloud increases with time of day and produces high accumulated rainfall during the early morning hours.

4 Conclusion

DSD characteristics associated with the ISM have been analyzed to understand the diurnal variation of DSD over the complex topography of the Western Ghats of India using the JWD observation collected between 2015 and 2019 at the HACPL, Mahabaleshwar. The gamma distribution of independent parameters, e.g., D_m and $\log_{10}N_{w,}$ along with other rain-integral parameters like R and Z, are also examined to understand the diurnal variation of DSD. Based on the analysis of the JWD measurements, the major findings are as follows:

1 With the rain rate and precipitating cloud type, the relationship between N(D) and D_m significantly alters. The gamma distribution broadens as the rate of rainfall increases.
2 Rain droplets of largest diameter growing in number and size, when moving from light to heavy precipitation for each time interval.
3 About 28.5% of rain events (23.6% of low rainfall and 4.9% of heavy rainfall) occurred during the 12-18 LST has highest contribution to the total accumulated rainfall.
4 The probability density function of D_m associated with the light and heavy precipitation demonstrated a substantial variance for each time interval (00-06, 06-12, 12-18, 18-23 LST).
5 The diurnal variation of R, Z, and $\log_{10}N_w$ demonstrated bimodal distribution, with a small peak around 5 LST and the highest peak in between 13-16 LST. At the same time, the $\log_{10}N_w$ diurnality reaches at its lowest value.
6 The hourly CAPE periodicity over the study region follows the diurnal variation of the rain-integral parameters.

Long-term measurement with high temporal resolution data has been utilized in the present study to determine how DSD changes throughout the day. In this study, we solely examined five years (2015–2019) of continuous ground-based JWD measurements taken during the monsoon season in the core region of the Western Ghats. However, adequate analyses are needed to comprehend the mechanics and thermodynamics of the atmospheric processes that cause DSD diurnality. Furthermore, the adequate representation of the diurnal variation of DSD in weather and climate models will help to improve the forecasting of rain intensity and duration over the Western Ghats, which is still challenging. Several hours before the actual timing, peak rainfall is

observed in the numerical models. Due to this, an imbalance in radiation equilibrium and dubious weather forecasting may possible. Precise numerical simulation of dynamical processes occurring between the land, ocean, and atmosphere can produce equivalent diurnal variation of DSD parameters.

Acknowledgements

The authors are thankful to the Director, IITM, Pune, for his encouragement and support throughout the study. Thanks are due to the use of Disdrometer data from the IITM-HACPL, Mahabaleshwar. Authors are thankful to the anonymous reviewers for their constructive comments and suggestions to improve the manuscript.

References

1 Marshall J S & Palmer W M K, *J Meteorol*, 5 (1948) 165.
2 Joss J & Waldvogel A, *J Atmos Sci*, 26 (1969) 566.
3 Jensen A A, Harrington J Y & Morrison H, *Mon Weather Rev*, 146 (2018) 723.
4 Boodoo S, *et al. J Hydrometeorol*, 16 (2015) 2027.
5 Angulo-Martínez M & Barros A P, *Geomorphology*, 228 (2015) 28.
6 Ulbrich C W & Atlas D, *J Appl Meteorol Climat*, 46 (2007) 1777.
7 Bringi V N, *et al., J Atmos Sci*, 60 (2003) 354.
8 Thurai M, Gatlin P N & Bringi V N, *Atmos Res*, 169 (2016) 416.
9 Tokay A & Short D A, *J Appl Meteorol*, 35 (1996) 355.
10 Houze R A, *Bull Am Meteorol Soc*, 78 (1997) 2179.
11 Konwar M, Das S K, Deshpande S M, Chakravarty K & Goswami B N, *J Geophys Res*, 119 (2014) 6140.
12 Das S K, Konwar M, Chakravarty K & Deshpande S M, *Atmos Res*, 186 (2017) 72.
13 Sumesh R K, Resmi E A, Unnikrishnan C K, Jash D & Ramachandran K K, *J Geophys Res Atmos*, 126 (2021) 1.
14 Das S K, *et al., Earth Space Sci*, 7 (2020) e2019EA000956.
15 Das S K, Krishna U V M, Kolte Y K, Deshpande S M & Pandithurai G, *Earth Space Sci*, 7 (2020).
16 Sreekanth T S, Varikoden H, Kumar M G & Resmi E A, *Sci Rep*, 9 (2019) 19083.
17 Sreekanth T S, Varikoden H, Resmi E A & Kumar M G, *Atmos Res*, 218 (2019) 90.
18 Murali K U V, Das S K, Deshpande S M, Doiphode S L & Pandithurai G, *Earth Space Sci*, 4 (2017) 540.
19 Murali K U V, *et al. Atmos Chem Phys*, 21 (2021) 4741.
20 Tawde S A & Singh C, *Int J Climatol*, 35 (2015) 2280.
21 Kumar A, Srivastava A K, Chakravarty K & Srivastava M K, *Pure Appl Geophys*, 179 (2022) 3875.
22 Harikumar R, Sampath S & Sasi K V, *Adv Space Res*, 45 (2010) 576.
23 Tokay A, Bashor P G & Wolff K R, *J Atmos Ocean Technol*, 22 (2005) 513.
24 Hersbach H, *et al., Q J R Meteorol Soc*, 146 (2020) 1999.
25 Krishna U V M, Das S K, Deshpande S M & Pandithurai G, *Sci Rep*, 11 (2021) 1
26 Basu B K, *Mon Weather Rev*, 135 (2007) 2155.